ELSEVIER

Chemical Engineering Journal 117 (2006) 131–136

Chemical Engineering Journal

www.elsevier.com/locate/cej

Sensitivity of process efficiency to reaction routes in exhaust-gas reforming of diesel fuel

A. Tsolakis [a,*], S.E. Golunski [b]

[a] *School of Engineering, Mechanical and Manufacturing Engineering, The University of Birmingham, Birmingham B15 2TT, UK*
[b] *Johnson Matthey Technology Centre, Blount's Court, Sonning Common, Reading RG4 9NH, UK*

Received 14 October 2005; received in revised form 12 December 2005; accepted 20 December 2005

Abstract

A catalytic exhaust-gas reformer is a largely passive reactor, which has to be capable of operating effectively at flow rates and inlet temperatures determined by the internal combustion engine. In this study, we examine the limited number of design parameters that can allow us to maximise the engine-reformer system efficiency while improving vehicle emissions. In principle, this balance requires that the endothermic hydrogen-generating reactions (steam reforming and dry reforming) are promoted at the expense of the exothermic reactions (oxidation, water-gas shift and methanation). In practice, an oxidation function is necessary for generating heat to drive the endothermic reactions, particularly at low exhaust gas temperatures. Water-gas shift and methanation respond to changes in size and aspect ratio of the reformer, but the ideal configuration for suppressing these CO-consuming reactions does not favour the efficient endothermic reactions at all operating conditions. Our results imply that the optimum exhaust-gas reformer cannot be achieved through reactor engineering alone, but will require further catalyst design.

Keywords: Fuel reforming; Internal combustion; Monolith catalysts; Exhaust gas recirculation

1. Introduction

The concept of on-board reforming dates back to the oil crisis of the 1970s, when it was considered as a means of promoting fuel-efficient lean combustion [1]. More recently, it has undergone extensive development as a potential hydrogen-generation technology for fuel cell powered vehicles [2,3]. However, since the move toward the use of hydrogen as the primary fuel for mobile fuel cells, on-board reforming is once again being targeted mainly at conventional vehicles [4,5]. Among the most promising technologies is a combination of reforming and exhaust-gas recirculation (referred to as *REGR*), which allows the fuel/air feed to the engine to be enriched with reformate (Fig. 1). When REGR is coupled with a diesel engine, the most notable effect is the simultaneous reduction in NO_x and particulate release, which is contrary to the expected tradeoff between these emissions [6].

Recent results [7] have shown that, in common with autothermal reforming of hydrocarbons [8], the main reactions during exhaust-gas reforming of diesel fuel are combustion (Eq. (1)), steam reforming (Eq. (2)), water-gas shift (Eq. (3)), and sometimes dry reforming (Eq. (4)), but as yet there is no conclusive evidence of direct partial oxidation (Eq. (5)) taking place. The different reactions can occur consecutively, resulting in distinctive temperature profiles along the length of the catalyst bed [9].

$$C_nH_{1.88n} + 1.47nO_2 \rightarrow nCO_2 + 0.94nH_2O \quad \Delta H = -8903\,\text{kJ/mol} \tag{1}$$

$$C_nH_{1.88n} + nH_2O \rightarrow nCO + 1.94nH_2 \quad \Delta H = +2492\,\text{kJ/mol} \tag{2}$$

$$mCO + mH_2O \rightarrow mCO_2 + mH_2 \quad \Delta H = -41.2\,\text{kJ/mol} \tag{3}$$

$$C_nH_{1.88n} + nCO_2 \rightarrow 2nCO + 0.9nH_2 \quad \Delta H = +2887\,\text{kJ/mol} \tag{4}$$

$$C_nH1.88n + \tfrac{n}{2}O_2 \rightarrow nCO + 0.94nH_2 \quad \Delta H = -1237\,\text{kJ/mol} \tag{5}$$

* Corresponding author. Tel.: +44 121 414 4170; fax: +44 121 414 7484.
E-mail address: a.tsolakis@bham.ac.uk (A. Tsolakis).

1385-8947/$ – see front matter © 2006 Elsevier B.V. All rights reserved.
doi:10.1016/j.cej.2005.12.017

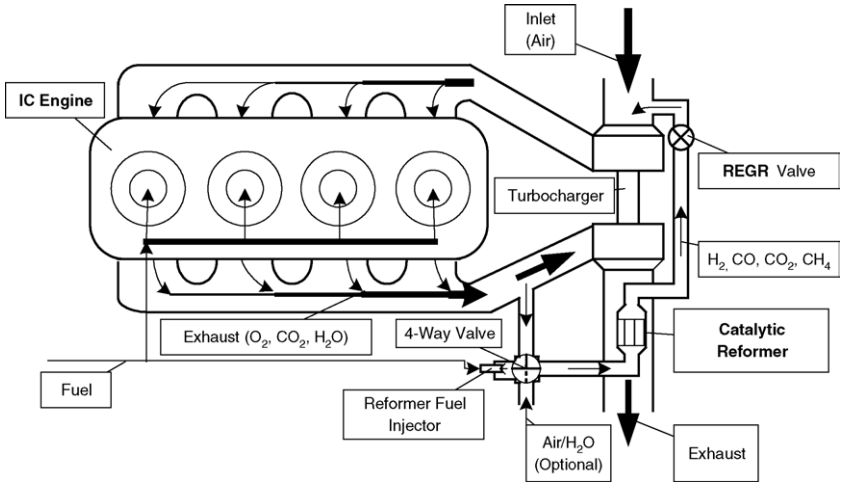

Fig. 1. Major components of REGR system.

Engine tests using different REGR compositions indicate [10] that it is not always desirable to optimise the hydrogen-generating reactions, and that the H_2 concentration need not be very high ($\leq$25% at the reformer outlet). In particular, unlike fuel-processing in fuel cell systems [11], there is not necessarily an advantage in converting as much CO as possible by reaction with steam. For example, the water-gas shift reaction increases the H_2 concentration, but it lowers the calorific value of the reformate. During REGR, the combustion of reformate that contains both CO and H_2 gives better overall fuel economy, while retaining the emission benefits seen by adding hydrogen alone [10].

In earlier publications we have shown that the steady-state performance of a reformer is affected by the nature of the diesel fuel [6,9,12,13], the exhaust gas conditions (dependent on the engine load) [6,10,12], and the configuration of the catalyst bed [9]. In the present work, we have observed how the reaction profiles in a monolith reforming catalyst respond to different reactant stoichiometries and space velocities, which are intended to mimic conditions during use of an REGR system when the engine is running at part load. The reaction profiles have allowed us to make correlations between the occurrence of specific reforming reactions and the overall efficiency of the reforming process. These correlations highlight the aspects of reactor and catalyst design that are most critical to the process of optimising exhaust-gas reforming.

2. Experimental

A catalyst with known resistance to carbon formation (nominal composition: 1% Rh/CeO_2-ZrO_2 by weight) was prepared by impregnating 50 g of 50:50 (mol basis) ceria-zirconia powder with 30 cm^3 of an aqueous solution of rhodium nitrate (containing 0.5 g rhodium). The impregnated powder formed a slurry, which was dried at 120 °C for 8 h, before being calcined in static air at 500 °C for 2 h. The catalyst was made into an aqueous suspension, which was uniformly coated onto ceramic monolith substrates with a high cell density (900 cpsi). The substrates were cylindrical (dia = 15 mm) with an aspect ratio (AR = length/diameter) of 10. This reactor configuration was of the type developed for hydrogen generation in fuel cell systems. Temperature profiles were obtained by slowly withdrawing a fine thermocouple along the length of a central monolith channel in the catalyst bed.

The effect of GHSV (the volumetric flow rate of the reactant feed divided by the external volume of the monolith catalyst) on the reaction profiles was examined at two different $H_2O/O_2/C$ ratios (Table 1). We did this by injecting fuel at two different feed rates into a synthetic exhaust gas containing a fixed ratio of air and steam at 290 °C, which mimicked the output from a diesel engine operating at part load. The injector was positioned 10 cm upstream of the catalyst, allowing the fuel to vaporize and mix with the synthetic exhaust gas before reaching the front face of the monolith. The fuel was ultra low sulphur diesel (average molecular formula: $C_{15}H_{28}$) with a cetane number of 53.9, which contained 24.4% aromatics and 46 mg kg^{-1} sulphur. Analysis of the product gas-stream included continuous measurement of carbon dioxide, carbon monoxide (both by non-dispersive IR), total hydrocarbons (FID) and oxygen (electrochemical method); the hydrogen and methane concentrations were measured by gas chromatography. The full test rig has been described in detail in a previous publication [6].

The theoretical reactor product gas concentrations for each operating condition were calculated using the STANJAN equilibrium model (v 3.89, Stanford University). The calculations were performed at constant pressure and temperature. The temperature used was equal to the maximum reaction temperature measured along the monolith for each test during steady-state reforming.

The process efficiency η was defined as the chemical power (kW) of the product stream divided by the chemical power of the diesel fuel in the feed:

$$\eta\,(\%) = \frac{\mathrm{LCV}_{\mathrm{fuel\,prod}}\dot{m}_{\mathrm{fuel\,prod}}}{\mathrm{LCV}_{\mathrm{fuel\,in}}\dot{m}_{\mathrm{fuel\,in}}} \times 100 \quad (6)$$

where $\mathrm{LCV}_{\mathrm{fuel\,prod}}$ and $\mathrm{LCV}_{\mathrm{fuel\,in}}$ are the lower calorific values of the combustible products (i.e. H_2, CO and CH_4) and the diesel fuel, respectively, and $\dot{m}_{\mathrm{fuel\,prod}}$ and $\dot{m}_{\mathrm{fuel\,in}}$ are the

Table 1
Test conditions

GHSV (h^{-1})	O/C: 1.88, O_2/C: 0.73, H_2O/C: 0.42				O/C: 1.43, O_2/C: 0.56, H_2O/C: 0.31			
	P_{input} (kW)	H_2O_{liquid} (ml h^{-1})	Air (l min^{-1})	$Fuel_{liquid}$ (ml h^{-1})	P_{input} (kW)	H_2O_{liquid} (ml h^{-1})	Air (l min^{-1})	$Fuel_{liquid}$ (ml h^{-1})
9200	0.27	12	2.3	24	0.35	12	2.3	36
13800	0.44	21	4.3	45	0.58	21	4.3	64
16100	0.54	24	5.3	57	0.71	24	5.3	77
18500	0.63	28	6.3	68	0.83	28	6.3	91

corresponding mass-flow rates. The predicted efficiency was calculated from the equilibrium product composition expected at the maximum temperature reached in the catalyst bed for each set of inlet conditions.

The reactor contact time (τ) (Eq. (7)) was calculated as the ratio of the monolith volume ($V_{Monolith}$) to the total volumetric gas flow ($\dot{V}_{Gas\ Flow}$) at the reactor inlet.

$$\tau = \frac{V_{Monolith}}{\dot{V}_{Gas\ Flow}} \quad (7)$$

This could be sub-divided into specific contact times for different axial zones in the monolith catalyst.

3. Results and discussion

3.1. Equilibrium models

When the maximum temperature in the catalyst bed is below 400 °C, equilibrium calculations predict that the major products of exhaust-gas reforming of diesel fuel are going to be CH_4 and CO_2 (Fig. 2). As the bed temperature rises, both these products are expected to decline sharply, while the concentrations of CO and H_2 increase. For an O/C ratio of 1.88, the equilibrium H_2 concentration reaches a peak of 19% at 650 °C, before declining very gradually over the next 650° (Fig. 2a). At the lower O/C ratio of 1.43, a similar pattern is predicted, but the maximum H_2 concentration is 23% (Fig. 2b).

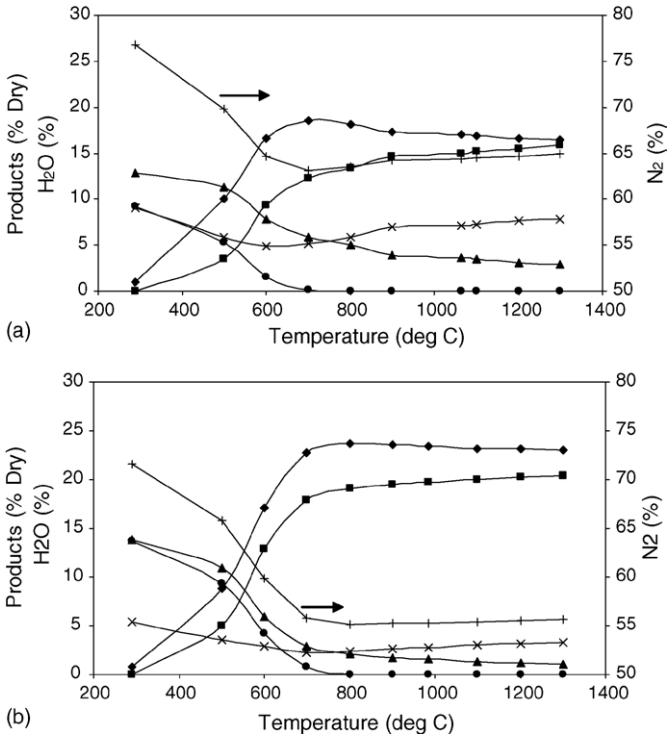

Fig. 2. Equilibrium product distribution predicted for exhaust-gas reforming of diesel fuel (a) O_2/C: 0.56, H_2O: 0.31 and O/C: 1.43; (b) O_2/C: 0.73, H_2O/C: 0.42 and O/C: 1.88. H_2 (♦), CO (■), CO_2 (▲), CH_4 (●) H_2O (×) N_2 (+).

3.2. Temperature profiles

Even during steady-state reforming, the temperature was non-uniform along the length of the catalyst bed. In the high aspect-ratio bed (long and thin) used in this study, this gave rise to a distinctive and stable profile, in which the temperature rose steeply to a peak (close to the inlet face of the bed) before declining much more gradually. The onset of this peak was associated with a rapid decline in gas-phase oxygen, indicating that the diesel fuel was oxidising as soon as it came into contact with the catalyst. Some of the heat was back-radiated, so that the gas temperature in the 2 cm preceding the catalyst bed was often 300–400 °C higher than the gas-feed temperature (290 °C in our tests).

The height, width and position of the peak responded to changes in the gas feed (Fig. 3). With increasing space velocity, the maximum temperature rose, and the peak shifted further along the catalyst bed. As the post-peak rate of temperature decline (°C/cm of bed) was very similar in each case, the highest space velocity resulted in the highest outlet temperature. For a fixed space velocity, lowering the O/C ratio caused a reduction in the peak height, but it did not have an affect on the outlet temperature (Fig. 4).

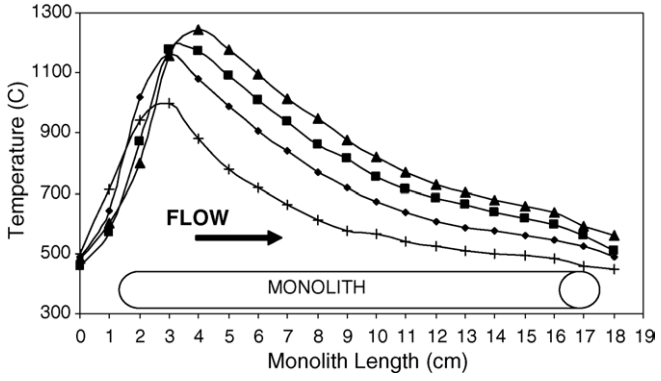

Fig. 3. Reactor temperature profile, at GHSV (h^{-1}): 9200 (+), 13800 (♦), 16100 (■), 18500 (▲); O/C ratio = 1.88.

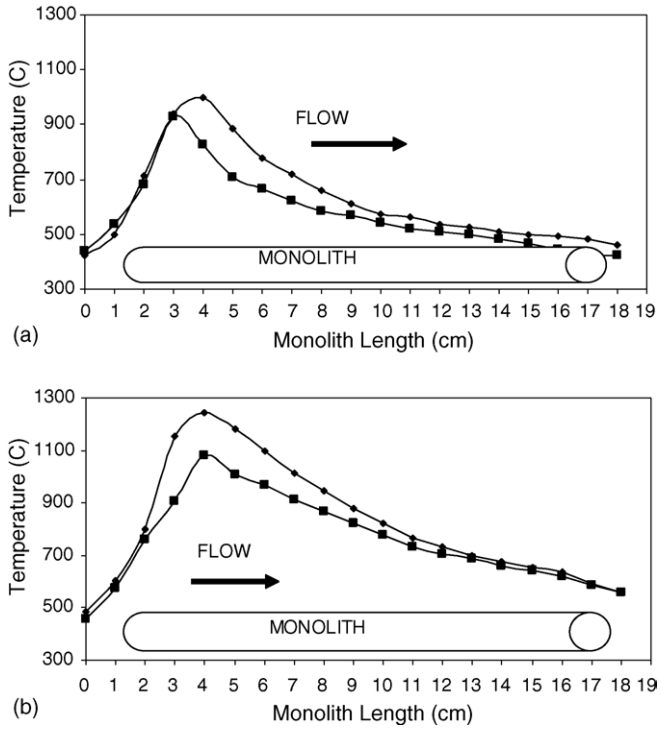

Fig. 4. Reactor temperature profile at (a) GHSV = 9200 h^{-1}, (b) GHSV: 18,500 h^{-1}; O/C ratio = 1.43 (■) and 1.88 (♦).

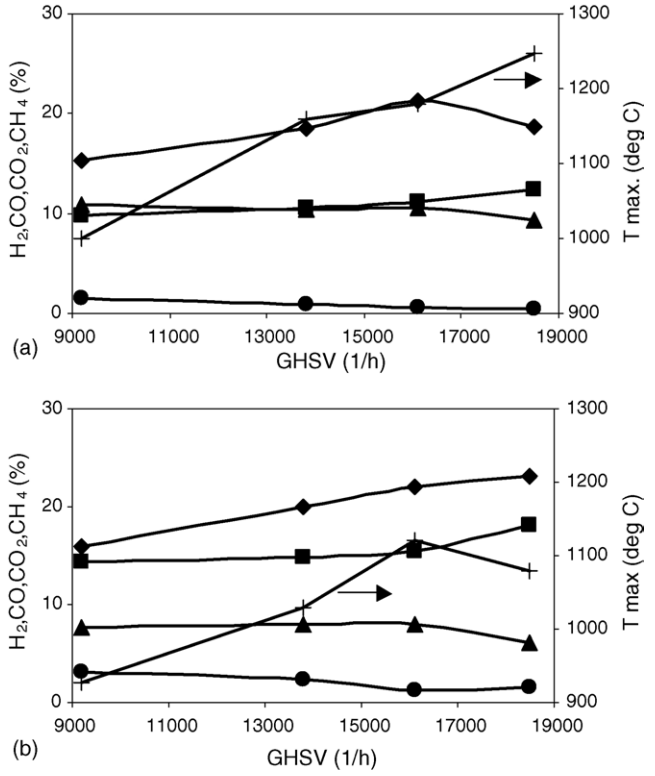

Fig. 6. Measured product distribution (a) O_2/C: 0.73, H_2O: 0.42 and O/C: 1.88; (b) O_2/C: 0.56, H_2O/C: 0.31 and O/C: 1.43. H_2 (♦), CO (■), CO_2 (▲), CH_4 (●) and temperature (+).

The effect of space velocity on the peak height is consistent with the most exothermic reactions being mass-transfer limited. Increasing the space velocity improves the transport of reactants to the active sites on the catalyst surface, resulting in higher rates of oxidation. The associated exotherm in turn leads to an increase in the mass transfer coefficient, which is dependent on diffusivity and gas viscosity, both of which change as a function of temperature [14]. Compared to the typical flat profile for a simple exothermic reaction in an adiabatic ceramic bed [15], the relatively steep decline in temperature is indicative of a consecutive endothermic reaction.

The stepwise increase in space velocity from 9200 to 18,500 h^{-1} corresponded to an overall decrease in contact time (τ) from 0.38 to 0.21 s. However, the contact time for the gas-stream in the portion of the catalyst bed above 700 °C (Fig. 5a) was surprisingly constant (except at the lowest space velocity at an O/C ratio of 1.43). We had chosen 700 °C as an approximate boundary temperature between that part of the bed in which the dominant H_2-producing reactions for a rhodium catalyst are likely to be dry reforming and steam reforming, and the part in which we expected water-gas shift to predominate. As the position of the temperature peak moved along the bed, the contact time for the portion below 700 °C decreased as a function of space velocity (Fig. 5b).

3.3. Product distribution

In general, when oxidation of the fuel was promoted by increasing the space velocity (i.e. improving the mass transfer), the increase in size of the temperature peak and its shift along the catalyst bed were accompanied by higher concentrations of H_2 in the product stream (Fig. 6). At first sight this seems consistent with the output coming closer to equilibrium, as the rate of the endothermic reforming reactions increase with the rise in bed temperature. However, the below-equilibrium CO and above-equilibrium H_2 and CO_2 concentrations at O/C = 1.88 (Table 2a) indicate that there is a substantial contribution from the water-

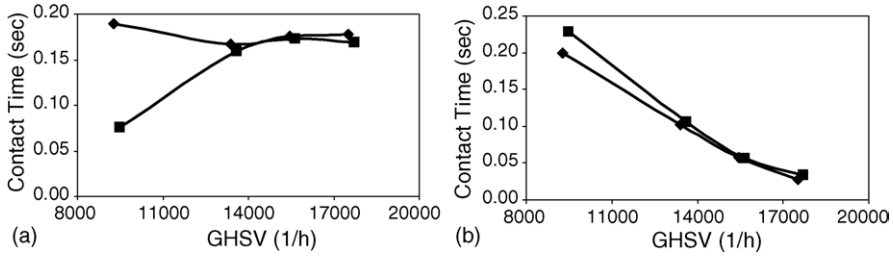

Fig. 5. Contact time (a) $\tau_{T>700\,^\circ C}$ and (b) $\tau_{T<700\,^\circ C}$ at different GHSV; O/C ratio = 1.88 (♦) and 1.43 (■).

Table 2
Actual and equilibrium concentrations for different GHSV at (a) O/C = 1.88 and (b) O/C = 1.43

GHSV (h^{-1})	T_{max} (°C)	P_{input} (kW)	H_2 (%)	$H_{2\,eq.}$ (%)	CO (%)	$CO_{eq.}$ (%)	CO_2 (%)	$CO_{2\,eq.}$ (%)	CH_4 (%)	$CH_{4\,eq.}$ (%)
(a) O/C = 1.88										
9200	1000	0.27	15.3	14.7	9.9	13.2	10.9	6.6	1.1	0.0
13800	1160	0.44	18.6	14.9	10.6	14.9	10.4	3.7	0.6	0.0
16100	1180	0.54	21.2	15	11.2	15	10.5	3.6	0.2	0.0
18500	1245	0.63	18.7	14.4	12.2	15	9.3	3.6	0.2	0.0
(b) O/C = 1.43										
9200	925	0.35	15.9	24.5	14.5	19.8	7.7	1.5	3.2	0.0
13800	1030	0.58	20.0	24.0	14.8	20.4	8.0	1.6	2.3	0.1
16100	1120	0.71	22.0	23.2	15.4	19.5	7.9	1.7	1.2	0.0
18500	1080	0.83	23.1	23.2	18.2	19.4	6.1	1.7	1.1	0.0

Equilibrium values calculated at the maximum temperature reached in the catalyst bed.

gas shift reaction, which takes place in the cooler zone (<700 °C) of the catalyst bed. Similarly, at O/C = 1.43, the CO concentrations were lower and the CO_2 higher than calculated, but now the H_2 did not exceed the equilibrium concentration (Table 2b). Instead, 1–3.2% CH_4 (i.e. 3–9.6% H_2-equivalent) was detected in the product stream, implying that hydrogen-formation was competing with methanation ($CO + 3H_2 \rightarrow CH_4 + H_2O$) in the cooler zone.

The simple relationship between maximum bed temperature and H_2 concentration only broke down at the highest space velocity with the higher O/C ratio (Fig. 6a). Under these conditions, with the peak temperature at 1245 °C (2 cm from the inlet face), the water-gas shift reaction could be constrained either kinetically by the low contact time in the cooler zone, or thermodynamically by the relatively high temperature throughout the bed (550 °C at the outlet). The kinetic effect seems more significant, as the product distribution did not come close to that predicted for equilibrium at the outlet temperature. Although ceria-supported rhodium is a recognised water-gas shift catalyst under exhaust-gas conditions [16], its optimum activity is restricted to a narrow range [17] that is limited at low temperature by low turnover frequency, and at high temperature by the predominance of the more thermodynamically favoured reverse-shift reaction. From the temperature profiles in Fig. 3, and the deviations from the expected equilibrium concentrations (Table 2a), we estimate that the optimum water-gas shift range for our catalyst was 550–700 °C.

The best process efficiency was achieved at the highest space velocity for O/C = 1.43 (Fig. 7). This coincided with the H_2 and CO concentrations coming closest to the predicted equilibrium values (Table 2b), and is consistent with the lowest contributions from the low-temperature exothermic reactions (water-gas shift and methanation). A similar effect was observed at O/C = 1.88, where the inefficient CO-consuming reactions were again suppressed as the cooler zone contracted with increasing space velocity. In principle, the greatest benefit to the process efficiency would come from dry reforming (Eq. (4)). However, the rhodium catalyst used in this study was surprisingly inactive for this reaction, as can be seen from the CO_2 concentrations, which were consistently higher than the equilibrium values, even after the contribution from water-gas shift is taken into account (Table 2).

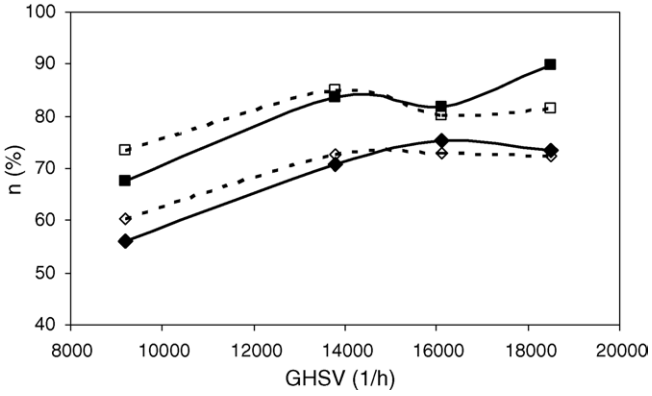

Fig. 7. Measured efficiency at O/C: 1.88 (♦) and O/C: 1.43 (■), and predicted efficiency at O/C: 1.88 (◊) and O/C: 1.43 (□).

4. Conclusions—reformer design implications

In a monolith reactor containing a rhodium catalyst, exhaust-gas reforming of diesel fuel takes place mainly through a combination of oxidation and steam reforming. Although the oxidation reactions generate an exotherm close to the inlet face, the onset of the endothermic H_2-generating reaction reverses the temperature rise, resulting in a characteristic asymmetric-peak profile along the length of the reactor. The catalyst has high intrinsic activity, allowing it to come close to equilibrium in the hot zone, once any mass transfer limitations have been overcome. In the cooler zone of the reactor, water-gas shift and CO-methanation become thermodynamically favoured. The catalyst is active for both these reactions, but the extent of their contributions is determined by the position and size of the temperature peak in the catalyst bed.

Currently, the design criteria for fuel reformers are still largely set by the requirements of polymer electrolyte fuel cell systems [18], which need a gas-stream that contains a high concentration of H_2 and virtually no CO. The hydrogen concentration has to be as high as possible, because the presence of any 'diluent' impacts on the hydrogen conversion in the fuel cell [19], while CO has a direct poisoning effect on the anode catalyst [20]. This means that water-gas shift is an integral part of the fuel-cell reforming process, which is usually coupled with

a preferential oxidation unit to remove the last traces of CO [21].

In exhaust-gas reforming, the key requirement is the efficient on-demand generation of a reformate containing only a relatively low concentration of H_2 (typically $\leq$20%) [6,12]. For an average exhaust temperature of 290 °C, the rhodium catalyst used in this study shows fast lightoff when diesel fuel is injected into the inlet stream. High reforming efficiency is achieved when the O/C inlet ratio is kept low and the low-temperature CO-consuming reactions are minimised. In principle, these slow and inefficient reactions can be avoided by reducing the length of the catalyst bed. However, on board a vehicle, an exhaust-gas reformer will have to function over a vast range of space velocities, and so the bed will have to be long enough to accommodate the axial movement of the high temperature peak. This means that the process efficiency will always suffer at low space velocity, where the peak is closest to the inlet face, and where much of the bed is available for the less efficient exothermic reactions. Therefore, the process of optimising exhaust-gas reforming technology will need to include further design of the catalyst as well as the reactor. For optimum fuel-economy, the catalyst should be capable of oxidation, dry reforming and steam reforming, but should have low activity for water-gas shift and methanation.

Acknowledgments

The authors would like to thank Johnson Matthey Plc. and Shell Global Solutions UK for their support for this work.

References

[1] Y. Jamal, M.L. Wyszynski, On-board generation of hydrogen-rich gaseous fuels—review, Int. J. Hydrogen Energy 19 (1994) 557.
[2] D.L. Trimm, Z.I. Onsan, On-board fuel conversion for hydrogen fuel cell driven vehicles, Catal. Rev. Sci. Eng. 43 (2001) 31.
[3] A. Faur Ghenciu, Review of fuel processing catalysts for hydrogen production in PEM fuel cell systems, Curr. Opin. Solid State Mater. Sci. 6 (2002) 389.
[4] P. Marsh, I. Gottberg, K. Thorn, M. Lundgren, F. Acke, G. Wirmark, SULEV emission technologies for a five-cylinder N/A engine. SAE Technical Paper 2000-01-0894.
[5] J.E. Kirwan, A.A. Quader, M.J. Grieve, Fast start-up on-board gasoline reformer for near-zero emissions in spark-ignition engine. SAE Technical Paper 2002-01-1011.
[6] A. Tsolakis, A. Megaritis, M.L. Wyszynski, Applications of the exhaust gas fuel reforming in compression ignition engines fuelled by diesel and biodiesel fuel mixtures, Energy Fuels 17 (2003) 1464.
[7] A. Tsolakis, A. Megaritis, Catalytic exhaust gas fuel reforming for diesel engines-effects of water additions on hydrogen production and fuel conversion efficiency, Int. J. Hydrogen Energy 29 (2004) 1409.
[8] D.L. Trimm, A. Adesina, Praharso, N.W. Cant, The conversion of gasoline to hydrogen for on-board vehicle applications, Catal. Today 93 (2004) 17.
[9] A. Tsolakis, A. Megaritis, S.E. Golunski, Reaction profiles during exhaust-assisted reforming of diesel engine fuel, Energy Fuels 19 (2005) 744.
[10] A. Tsolakis, A. Megaritis, D. Yap, A. Abu-Jrai, Combustion characteristics and exhaust gas emissions of diesel engine supplied with reformed EGR. SAE Technical Paper 2005-01-2087.
[11] A.K. Avci, Z.I. Onsan, D.L. Trimm, On-board fuel conversion for hydrogen fuel cells: comparison of different fuels by computer simulations, Appl. Catal. A: Gen. 216 (2001) 243.
[12] A. Tsolakis, A. Megaritis, Partially premixed charge compression ignition engine with on-board hydrogen production by exhaust gas fuel reforming of diesel and biodiesel, Int. J. Hydrogen Energy 30 (2005) 731.
[13] A. Tsolakis, A. Megaritis, Exhaust gas assisted reforming of rapeseed methyl aster for reduced exhaust emissions of CI engines, Biomass Bioenergy 27 (2004) 493.
[14] H. Scott Fogler, Elements of Chemical Reaction Engineering, Prentice-Hall International, New Jersey, 1992, p. 565.
[15] D.W. Flick, M.C. Huff, Oxidative dehydrogenation of ethane over a Pt-coated monolith versus monolith Pt-loaded pellets: surface area and thermal effects, J. Catal. 178 (1998) 315.
[16] J. Barbier Jr., D. Duprez, Reactivity of steam in exhaust gas catalysis I. Steam and oxygen/steam conversions of carbon monoxide and of propane over PtRh catalysts, Appl. Catal. B: Environ. 3 (1993) 61.
[17] B.I. Whittington, C.J. Jiang, D.L. Trimm, Vehicle exhaust catalysis: I. The relative importance of catalytic oxidation, steam reforming and water-gas shift reactions, Catal. Today 26 (1995) 41.
[18] S. Ahmed, M. Krumpelt, Hydrogen from hydrocarbon fuel for fuel cells, Int. J. Hydrogen Energy 26 (2001) 291.
[19] G.J.M. Janssen, Modelling study of CO_2 poisoning on PEMFC anodes, J. Power Sources 136 (2004) 45.
[20] T.R. Ralph, M.P. Hogarth, Catalysis for low temperature fuel cells, Platinum Met. Rev. 46 (2002) 117.
[21] A. Manasilp, E. Gulari, Selective CO oxidation over Pt/Alumina catalyst for fuel cell applications, Appl. Catal. B: Environ. 37 (2002) 17.